CSPS | jpps Journal of Pharmacy and Pharmaceutical Sciences

TYPE Original Research
PUBLISHED 24 November 2026
DOI 10.3389/jpps.2026.17135

Check for updates

OPEN ACCESS

EDITED BY
Khaled Naja,
Qatar University, Qatar

*CORRESPONDENCE
Khaoula Errafii,
khaoula.errafii@adu.ac.ae

RECEIVED 13 June 2026
REVISED 09 October 2026
ACCEPTED 20 October 2026
PUBLISHED 24 November 2026

CITATION
Errafii K, Hamdi A and Abu Obaid A (2026) LncRNA profiling identifies transcriptional dysregulation in human white adipose tissue associated with hyperinsulinaemic insulin resistance.
J. Pharm. Pharm. Sci. 29:17135.
doi: 10.3389/jpps.2026.17135

COPYRIGHT
© 2026 Errafii, Hamdi and Abu Obaid. This is an open-access article distributed under the terms of the Creative Commons Attribution License (CC BY). The use, distribution or reproduction in other forums is permitted, provided the original author(s) and the copyright owner(s) are credited and that the original publication in this journal is cited, in accordance with accepted academic practice. No use, distribution or reproduction is permitted which does not comply with these terms.

LncRNA profiling identifies transcriptional dysregulation in human white adipose tissue associated with hyperinsulinaemic insulin resistance

Khaoula Errafii*, Amel Hamdi and Asmaa Abu Obaid

Department of Biomedical Sciences, College of Health Sciences, Abu Dhabi University, Abu Dhabi, United Arab Emirates

Long non-coding RNA (lncRNA) expression in human white adipose tissue (WAT) remains incompletely characterised in hyperinsulinaemic insulin resistance without diagnosed diabetes. We performed a cross-sectional analysis of genome-wide lncRNA expression in subcutaneous WAT from 24 participants: lean healthy controls (n = 8), obese participants with hyperinsulinaemic insulin resistance without diagnosed diabetes (Obese-IR, n = 8; fasting insulin ≥9 mU/L and elevated HOMA-IR), and obese participants with type 2 diabetes (Obese-T2D, n = 8). Our analyses included differential expression, expression-based co-expression profiling, exploratory biomarker assessment, and genomic proximity-based identification of putative cis-target genes. PERMANOVA detected significant differences in lncRNA expression profiles across the three groups ($F = 1.383$, $R^2 = 0.116$, $p = 0.025$), including between lean and Obese-IR participants ($F = 1.673$, $R^2 = 0.107$, $p = 0.0002$). Compared with lean controls, 128 lncRNAs were differentially expressed in Obese-IR participants and 408 in Obese-T2D participants. Thirty-two lncRNAs were shared between these comparisons, demonstrating complete directional concordance and strongly correlated $\log_2$ fold changes (Pearson $r = 0.969$, $p < 0.0001$). Pathway and network analyses of putative cis-target genes highlighted processes related to lipid metabolism, inflammatory signalling, insulin signalling, and PPARG-associated adipogenesis. Expression-based co-expression analysis identified five lncRNA clusters. FAM95A and LINC01230 showed exploratory discriminatory performance for lean versus Obese-IR participants, with AUCs of 0.867 (95% CI 0.675–1.000) and 0.828 (95% CI 0.593–1.000), respectively. These findings identify both shared and comparison-specific lncRNA expression patterns in human WAT, including differences observed in hyperinsulinaemic insulin-resistant participants without diagnosed diabetes. Independent validation, longitudinal studies, and functional experiments are required to establish their predictive value, temporal relationships, and causal regulatory roles.

KEYWORDS
hyperinsulinemia, lncRNA, obesity, transcriptomics, white adipose tissue

Introduction

Type 2 diabetes mellitus (T2D) and its associated metabolic comorbidities represent one of the most significant and rapidly growing threats to global health [1]. Analysis of the Global Burden of Disease 2021 dataset demonstrates that T2D has increased at an accelerating rate of 0.42% annually over the past three decades and now accounts for 75 million disability-adjusted life years worldwide [2]. While the molecular pathophysiology of T2D is multifactorial, white adipose tissue (WAT) dysfunction occupies a central and causally upstream position in disease progression [3]. Adipose tissue is an active endocrine and transcriptionally dynamic organ whose dysfunction is central to the development of systemic insulin resistance and the progression of metabolic disease [3]. Adipose tissue alterations have been associated with insulin resistance in individuals with obesity, supporting the investigation of molecular differences in obese participants without diagnosed diabetes [4].

LncRNAs are a heterogeneous class of RNA molecules exceeding 200 nucleotides in length that lack significant protein-coding potential but exert diverse regulatory effects at the transcriptional, post-transcriptional, and epigenetic levels [3, 5]. LncRNAs regulate target gene expression through multiple mechanisms, including chromatin remodelling, transcription factor scaffolding, enhancer activation, RNA-protein complex formation, and cis-regulation of neighbouring protein-coding genes through genomic proximity [5–7]. The human genome encodes tens of thousands of lncRNA species, the vast majority of which exhibit tissue-restricted expression patterns [5, 7], with adipose tissue representing one of the most lncRNA-rich transcriptional environments in the body [8]. Despite this abundance, the functional characterisation of adipose lncRNAs in the context of insulin resistance and type 2 diabetes remains incomplete [8–10].

Emerging evidence implicates specific adipose lncRNAs in the regulation of adipocyte differentiation, lipid metabolism, and inflammatory signalling [7, 11, 12]. Beyond adipose tissue itself, lncRNA dysregulation and its link to inflammation and insulin resistance have also been reported in other insulin-resistant states. In a cross-sectional study of gestational diabetes mellitus (GDM), Dey et al. found that MALAT1, MEG3, and XIST were significantly downregulated in the peripheral blood of GDM patients compared with normoglycaemic pregnant controls, and that expression of all three lncRNAs correlated negatively with HOMA-IR and with the proinflammatory cytokines IL-6, IL-1β, and TNF-α. These findings support the broader principle that lncRNA downregulation tracks both worsening insulin resistance and heightened inflammatory tone across distinct insulin-resistant states, reinforcing the rationale for characterising the coordinated suppression of inflammation-linked lncRNAs that we have identified in insulin-resistant adipose tissue [13]. linc-ADAIN, identified in human white adipose tissue, regulates KLF5 and IL-8 mRNA stability through IGF2BP2 interaction; its knockdown in human adipose stromal cells increases adipocyte size and macrophage infiltration, directly reproducing hallmark features of obesity-induced adipose dysfunction [10] linc-GALNTL6-4, an adipocyte-specific lncRNA whose expression co-segregates with obesity and normalises upon weight loss, regulates adipogenesis and lipid homeostasis through modulation of APOC1 and triglyceride metabolism; its knockdown impairs adipogenesis, induces lipidomic alterations, and propels inflammation [9].

These examples demonstrate that individual adipose lncRNAs can function as critical regulatory nodes controlling multiple converging aspects of adipocyte biology [9, 10]. To our knowledge, no published study has comprehensively characterised the lncRNA transcriptome of human white adipose tissue across the full metabolic disease continuum, particularly in relation to the hyperinsulinaemic insulin-resistant phenotype in individuals without diagnosed diabetes [8, 14].

The genome-wide characterisation of adipose lncRNA expression in well-phenotyped obese subjects without diagnosed diabetes remains incomplete [14, 15]. The MD-Lipolysis cohort provides deep metabolic phenotyping, including OGTT, HOMA-IR, the Matsuda index, microdialysis, and adipose biopsy [16]. Characterising lncRNA expression alongside metabolic phenotyping provides a basis for examining associations with obesity and insulin resistance [15, 17]. The MD-Lipolysis cohort, as described by Fryk et al., includes obese participants without diagnosed diabetes with documented hyperinsulinaemia and elevated HOMA-IR [16]. This phenotype supports the investigation of adipose lncRNA expression in hyperinsulinaemic insulin resistance.

In the present study, we performed genome-wide lncRNA transcriptomics on subcutaneous WAT from 24 participants: lean healthy controls, obese participants with hyperinsulinaemic insulin resistance without diagnosed diabetes (Obese-IR), and obese participants with T2D (Obese-T2D). We identified 128 lncRNAs differentially expressed in the Obese-IR versus lean comparison, and 408 in the Obese-T2D versus lean comparison. Overlap analysis characterised shared and comparison-specific expression patterns, while pathway and network analyses of putative cis-target genes highlighted biological processes potentially associated with these differences. We additionally performed an expression-based hierarchical co-expression analysis and an exploratory, ROC-based assessment of candidate biomarkers. We also constructed a genomic proximity-based lncRNA–mRNA network. These analyses aimed to characterise adipose lncRNA expression across metabolic groups and identify candidates for subsequent validation.

Materials and methods

Data acquisition and preprocessing

This study was a cross-sectional secondary analysis of publicly available subcutaneous white adipose tissue RNA-sequencing data from 24 independent participants. The data were retrieved from the NCBI Gene Expression Omnibus (GEO; accession number GSE141432), with the raw sequencing reads accessible through the Sequence Read Archive (SRA; accession number SRP234695), corresponding to the MD-Lipolysis cohort described by [16]. The study included three metabolic groups: lean healthy controls (n = 8), obese participants with hyperinsulinaemic insulin resistance without diagnosed diabetes (Obese-IR, n = 8), and obese participants with type 2 diabetes (Obese-T2D, n = 8). In the source cohort, obese participants without diabetes were selected based on fasting insulin ≥9 mU/L, and insulin resistance was

characterised using HOMA-IR; OGTT and the Matsuda index provided additional metabolic phenotyping. The Obese-IR source cohort included two participants with impaired fasting glucose and one with impaired glucose tolerance. The label Obese-IR is therefore used rather than a label implying normal glucose tolerance, without assuming that every participant had normal glucose tolerance. These source-cohort counts are not assigned to the eight RNA-sequenced participants without participant-level linkage. The analyses compared different participants across groups and did not assess longitudinal changes within individuals.

Raw reads were quality-assessed using FastQC (v0.12.1) and adapter-trimmed using Trimmomatic (v0.39) [18]. The trimmed reads were aligned to the GRCh38 reference genome using STAR (v2.7.10b) in two-pass mode [19], with GENCODE v44 as the reference annotation [20]. Gene-level read counts were generated using featureCounts (Subread v2.0.3) [21] and filtered to retain lncRNA biotype features, yielding a final expression matrix of 34,914 lncRNA features across 24 samples.

Differential expression analysis

Differential expression analysis was performed using DESeq2 (v1.42.0) [22] in R (v4.3.1). Pairwise contrasts were computed between the Lean vs. Obese-IR and Lean vs. Obese-T2D groups. Significance thresholds were set at a false discovery rate (FDR) < 0.05 and $|\log_2$ fold change ($\log_2$FC)$| \geq 1$, with multiple testing correction applied using the Benjamini-Hochberg procedure. Variance-stabilised expression values were used for principal component analysis (PCA), and global group separation was formally evaluated by permutational multivariate analysis of variance (PERMANOVA; 9,999 permutations) using the vegan package (v2.6.4) in R [23].

Overlap and comparative analysis

To identify shared and comparison-specific patterns of lncRNA differential expression, an overlap analysis was performed between the Obese-IR versus lean and Obese-T2D versus lean DE lncRNA sets using custom scripts in Python (v3.11).

Three mutually exclusive groups were defined: IR-unique lncRNAs (significant in Lean vs. Obese-IR only), T2D-unique lncRNAs (significant in Lean vs. Obese-T2D only), and shared lncRNAs (significant in both comparisons). Directional concordance for shared lncRNAs was assessed by comparing the sign of $\log_2$FC across both contrasts. Pearson's correlation coefficient between IR and T2D $\log_2$FC values for shared lncRNAs was computed using scipy. stats.pearsonr (Python v3.11), with two-tailed p-values reported. The absolute fold-change ratio was calculated as the ratio $|\log_2$FC T2D$|/|\log_2$FC IR$|$ for each shared lncRNA. Visualisations, including Venn diagrams, bar charts, pie charts, and scatter plots, were generated using matplotlib (v3.7.2), seaborn (v0.12.2), and matplotlib-venn (v0.11.9) in Python v3.11.

Cis-target gene identification

Protein-coding cis-target genes were identified for each significantly DE lncRNA using a ±500 kb genomic window, consistent with established lncRNA putative cis-regulatory proximity thresholds [5, 6]. Chromosomal coordinates of all DE lncRNAs were extracted from GENCODE v44 annotations [20] and cross-referenced against all annotated protein-coding genes (biotype: protein_coding) within the same genomic interval using custom Python scripts. Where multiple DE lncRNAs shared a putative cis-target gene, the entry with the largest absolute $\log_2$FC was retained. All cis-target gene lists were deduplicated at the HGNC gene symbol level. The smaller number of unique cis-target protein-coding genes identified in the T2D-stage analysis (88 genes from 408 DE lncRNAs) relative to the IR-stage analysis (196 genes from 128 DE lncRNAs) may reflect the following factors. First, a higher proportion of T2D-stage DE lncRNAs are unannotated intergenic transcripts (74.0% carry only ENSEMBL identifiers versus 64.8% at the IR stage), which may indicate that they are located in gene-sparse genomic regions with fewer neighbouring protein-coding genes within ±500 kb. Second, the more extensive T2D lncRNA dysregulation includes genomically clustered transcripts that share cis-target genes; after deduplication, this convergence substantially reduces the number of unique cis-target genes. Third, the ±500 kb window is a permissive proximity threshold (1 Mb in total), which was adopted from published convention; it was not tested against narrower windows, so the cis-target sets may be sensitive to this choice (see Limitations).

For the IPA upload, the files were formatted as tab-delimited text with three columns: gene identifier (HGNC symbol), expression log ratio (lncRNA $\log_2$FC), and significance value (FDR p-value). Two separate cis-target gene sets were generated: 196 unique protein-coding genes for the IR-stage analysis and 88 unique protein-coding genes for the T2D-stage analysis, both achieving 100% mapping to the QIAGEN Knowledge Base.

Ingenuity pathway analysis

IPA Core Analysis was performed using QIAGEN Ingenuity Pathway Analysis [24] on two independent cis-target gene sets: 196 unique protein-coding genes from 128 IR-stage DE lncRNAs (100% mapped to the QIAGEN Knowledge Base) and 88 unique protein-coding genes from 408 T2D-stage DE lncRNAs (100% mapped). The analysis parameters were set to *Homo sapiens*, with the tissue filters restricted to adipose tissue, adipocytes, and 3T3-L1 cells, and the interaction confidence limited to experimentally observed and high-confidence predicted interactions. Canonical pathway enrichment was assessed using Fisher's exact test; pathways with $-\log_{10}(p) \geq 1.3$ (equivalent to $p < 0.05$) were considered significant. The predicted activation or inhibition state was evaluated using the IPA z-score algorithm, with $|z| \geq 2$ as the threshold for directional significance [25]. This analytical approach has been previously applied to characterise lncRNA cis-regulatory consequences in metabolic disease [24, 25].

Hierarchical co-expression analysis

Gene identifiers were harmonised between the differential expression results and the expression matrix, accounting for the "gene:" prefix attached to Ensembl identifiers in the matrix. All 128 lncRNAs differentially expressed in the Obese-IR versus lean comparison were matched. A detection threshold of a raw

count ≥1 in at least five of the 24 samples was used to retain 127 lncRNAs for co-expression analysis. ENSG00000176868 was excluded because it was detected in only three samples. Hierarchical clustering was performed using $\log_2$(CPM + 1) expression values, Pearson correlation distance, and average linkage, and the resulting dendrogram was partitioned into five modules. The Supplementary Data Sheet 1, sheet Cluster_assignments provides identifier mappings, detection counts, inclusion decisions, and module assignments.

Statistical analysis

Pearson's correlation coefficient was used to assess $\log_2$FC concordance between IR and T2D stages for shared lncRNAs, with two-tailed p-values reported. ROC analysis was performed on $\log_2$(CPM+1) expression values (CPM counts normalised to total lncRNA counts per sample) for pairwise group comparisons; AUCs were calculated from the rank-based (Mann–Whitney) statistic, with ties counted as one-half, and 95% confidence intervals were obtained using the DeLong method (normal approximation; limits truncated to the 0–1 range). Canonical pathway enrichment in IPA was assessed using Fisher's exact test; upstream regulator significance was evaluated by overlap p-value combined with activation z-score. A significance threshold of $p < 0.05$ was applied to all analyses unless otherwise stated.

Results

lncRNA expression profiles differ across lean, obese-IR, and obese-T2D groups

To determine whether lncRNA expression profiles differ systematically across metabolic states, we performed PCA on the full lncRNA transcriptome of 24 WAT samples, which spanned three metabolic groups: lean healthy controls, obese subjects with hyperinsulinaemic insulin resistance without diagnosed diabetes (Obese-IR), and obese subjects with overt T2D (Obese-T2D).

PC1 and PC2 together explained 27.0% of the total transcriptomic variance and revealed a partial separation of the three groups in lncRNA expression space (Figure 1A). Lean samples formed a discrete cluster, while Obese-IR and Obese-T2D samples occupied increasingly displaced positions along PC1, consistent with a gradient in expression profiles across the three groups. This separation was further confirmed in the PC1 versus PC3 projection (Figure 1B), which recapitulated the same group ordering and reinforced that the observed stratification is not confined to a single principal component.

PERMANOVA analysis indicated that metabolic group membership accounted for 11.6% of the variation in lncRNA expression profiles across the three groups ($F = 1.383$, $R^2 = 0.116$, $p = 0.025$). Pairwise analyses detected significant differences between lean and Obese-IR participants ($F = 1.673$, $R^2 = 0.107$, $p = 0.0002$) and between Obese-IR and Obese-T2D participants ($F = 1.339$, $R^2 = 0.087$, $p = 0.011$). The difference between lean and Obese-T2D participants did not reach statistical significance ($p = 0.176$). These results indicate differences in lncRNA expression profiles between metabolic groups without establishing a temporal sequence of transcriptomic changes.

Together, these findings indicate differences in lncRNA expression profiles among the metabolic groups and provide a basis for subsequent differential expression and pathway analyses. The Obese-IR comparison describes hyperinsulinaemic insulin resistance without diagnosed diabetes and does not establish a temporal transition towards T2D.

128 lncRNAs are significantly differentially expressed in obese-IR adipose tissue versus lean controls

To identify lncRNAs differentially expressed between lean participants and those with hyperinsulinaemic insulin resistance, we performed a differential expression analysis comparing WAT from lean healthy subjects (n = 8) to obese individuals with hyperinsulinaemic insulin resistance without diagnosed diabetes (Obese-IR, n = 8) across 34,914 lncRNA features. Applying a significance threshold of FDR < 0.05 and $|\log_2 FC| \geq 1$, we identified 128 significantly differentially expressed lncRNAs (Figure 2A). Of these, 77 were downregulated, and 51 were upregulated in Obese-IR adipose tissue relative to lean controls, indicating a predominance of downregulated lncRNAs in the Obese-IR group.

The volcano plot revealed a clear asymmetry in effect size between the two directions of dysregulation: downregulated lncRNAs exhibited greater fold changes and higher statistical significance, with several candidates reaching $-\log_{10}(\text{FDR}) > 10$, corresponding to FDR values below 10^{-10}. The most significantly downregulated candidates included FAM95A ($\log_2 FC = -5.67$, FDR < 0.001), SYBU-AS1 ($\log_2 FC = -4.57$, FDR < 0.001), LINC01230 ($\log_2 FC = -1.44$, FDR < 0.001), LINC01612 ($\log_2 FC = -2.89$, FDR < 0.001), and PARAL1 ($\log_2 FC = -2.53$, FDR < 0.001). The top 20 DE lncRNAs ranked by absolute fold change are shown in Figure 2B, spanning a $\log_2 FC$ range of −8.21 to 3.96 and comprising both named HGNC lncRNAs and novel GENCODE-annotated transcripts lacking current HGNC designation.

Notably, the predominance of downregulated lncRNAs in hyperinsulinaemic insulin-resistant adipose tissue is consistent with a repression-dominant expression pattern. This repressive signature, detectable in participants without diagnosed diabetes, provides a basis for subsequent exploratory pathway and network analyses.

Differential lncRNA expression in obese type 2 diabetic adipose tissue identifies both shared and diabetes-specific transcriptomic changes

To characterise the lncRNA transcriptome of overt T2D in white adipose tissue, and to define what is diabetes-specific versus what originates at the insulin-resistant stage, we performed a differential expression analysis comparing lean (n = 8) and Obese-T2D (n = 8) subjects across 34,914 lncRNA features using identical analytical criteria (FDR < 0.05, $|\log_2 FC| \geq 1$). A total of 408 lncRNAs were significantly differentially expressed in Obese-T2D adipose tissue relative to lean controls (Figures 3A,B), representing a 3.2-fold expansion relative to the 128 lncRNAs identified in the IR comparison. Strikingly, the directional profile of T2D lncRNA

10.3389/jpps.2026.17135

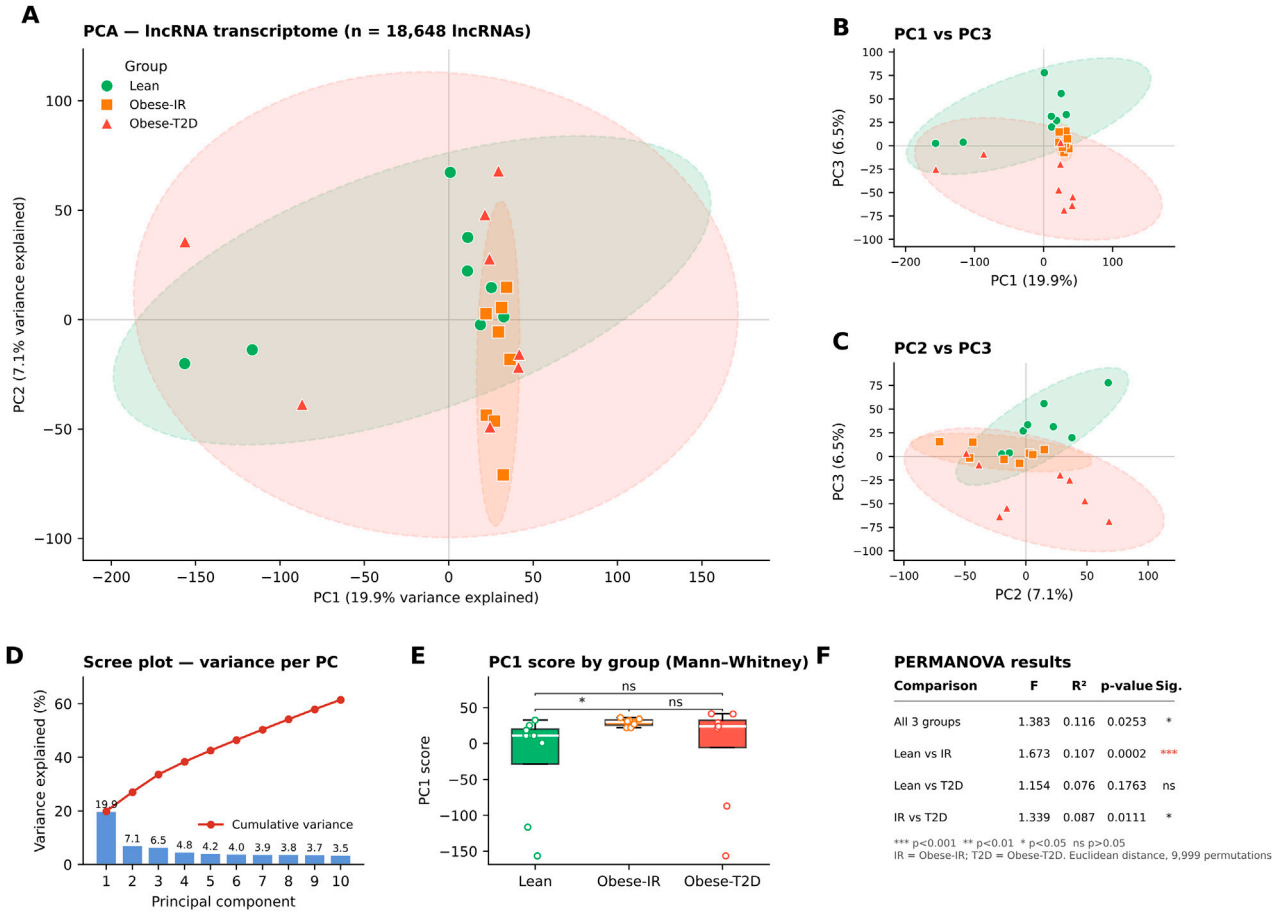


FIGURE 1
Principal component analysis (PCA) of the lncRNA transcriptome across lean, obese hyperinsulinaemic IR without diagnosed diabetes (Obese-IR), and obese type 2 diabetic (Obese-T2D) white adipose tissue. PCA was performed on variance-stabilized $\log_2$ counts per million ($\log_2$ (CPM)) expression values of 18,648 expressed lncRNAs across 24 subjects (Lean n = 8, Obese-IR n = 8, Obese-T2D n = 8). Each point represents one individual sample; shapes denote group (circle = Lean, square = Obese-IR, triangle = Obese-T2D). Shaded ellipses represent 95% confidence intervals. **(A)** PC1 (19.9% variance) versus PC2 (7.1% variance). (B) PC1 versus PC3 (6.5% variance), **(C)** PC2 versus PC3. **(D)** Scree plot of variance explained by the first ten principal components, with cumulative variance. **(E)** PC1 scores by group, with individual samples overlaid. **(F)** PERMANOVA results table (pseudo-F, R-squared, p-value; Euclidean distance, 9,999 permutations). Group separation was confirmed by permutation-based multivariate analysis of variance (PERMANOVA; 9,999 permutations): overall F = 1.383, R^2 = 0.116, p = 0.025; Lean vs. Obese-IR: F = 1.673, R^2 = 0.107, p = 0.0002; Obese-IR v. s T2D: F = 1.339, R^2 = 0.087, p = 0.011.

dysregulation was the inverse of that observed in insulin-resistant adipose tissue. While the IR stage was characterised by a predominantly repressive lncRNA signature, T2D showed a marked shift towards transcriptional activation, with 271 lncRNAs upregulated and 137 downregulated in Obese-T2D subjects relative to lean controls. This directional reversal from repression-dominant in insulin resistance to activation-dominant in T2D suggests a difference in the direction of lncRNA dysregulation between the Obese-IR and Obese-T2D groups.

The most statistically significant DE lncRNAs in T2D included several candidates also identified at the IR stage. The most significant single lncRNA was TRIM55 Antisense ($\log_2$FC = −7.85, FDR = 2.28×10^{-30}), which was also the top downregulated hit in the IR comparison, suggesting that it represents an lncRNA whose suppression is shared between the Obese-IR and Obese-T2D comparisons. Other highly significant candidates included LINC01612 ($\log_2$FC = −4.66, FDR = 2.27×10^{-14}), ENSG00000291250 ($\log_2$FC = −3.56, FDR = 1.66×10^{-12}), and SYBU-AS1 ($\log_2$FC = −5.23, FDR = 2.69×10^{-6}). Among the most upregulated candidates, ENSG00000310528 ($\log_2$FC = 5.09, FDR = 1.3×10^{-5}), LINC00570 ($\log_2$FC = 4.48, FDR = 4.9×10^{-4}), and MFSD12-AS1 ($\log_2$FC = 4.23, FDR = 3.2×10^{-3}) showed the greatest positive fold changes. The predominance of upregulated lncRNAs in T2D, in contrast to the downregulation bias in IR, suggests that the two groups differ in both the direction of lncRNA dysregulation and in its extent, as examined further in the overlap analysis in Section *Cis-target gene identification*.

Comparative analysis identifies shared and comparison-specific lncRNA expression patterns across metabolic groups

To identify shared and comparison-specific patterns of lncRNA differential expression, we performed an overlap analysis between the Obese-IR versus lean and Obese-T2D versus lean DE lncRNA

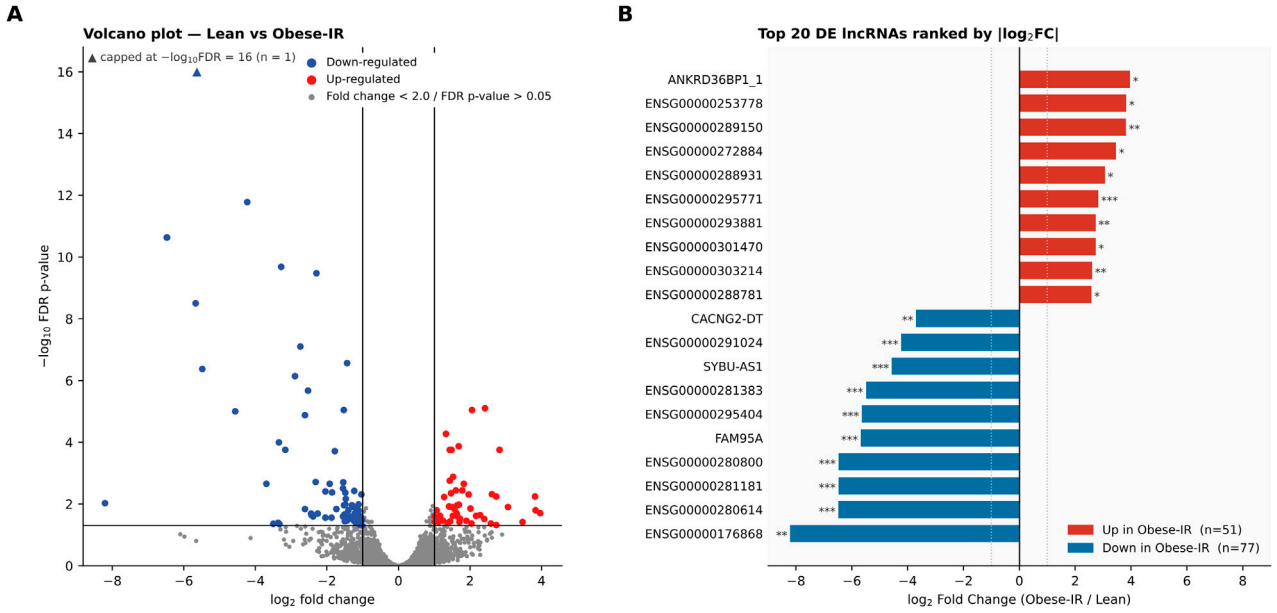


FIGURE 2
Differential lncRNA expression in white adipose tissue of hyperinsulinaemic insulin-resistant subjects relative to lean controls. **(A)** Volcano plot of lncRNAs tested for differential expression between lean (n = 8) and obese insulin-resistant (Obese-IR, n = 8) subjects. The x-axis shows $\log_2$ fold change (Obese-IR relative to Lean) and the y-axis shows $-\log_{10}$ FDR p-value. Vertical lines indicate the $|\log_2 FC| = 1$ threshold. **(B)** Horizontal bar chart of the top 20 differentially expressed lncRNAs ranked by absolute $\log_2$ fold change, comprising the 10 most upregulated and 10 most downregulated in Obese-IR relative to lean adipose tissue. Significance stars indicate FDR thresholds (* FDR < 0.05; ** FDR < 0.01; *** FDR < 0.001).

sets (Figure 4A). Of the 128 IR-stage DE lncRNAs, 96 (75.0%) were significant only in the Obese-IR versus lean comparison and did not meet the significance criteria in the Obese-T2D comparison. These lncRNAs are candidates for future experimental validation; the data do not show whether they precede or follow hyperglycaemia. A conserved core of 32 lncRNAs (25.0% of IR; 7.8% of T2D DE genes) was shared between the two comparisons, with the remaining 376 lncRNAs (92.2%) significant only in the Obese-T2D versus lean comparison, indicating that many more lncRNAs met the criteria only in the Obese-T2D comparison (Figure 4A).

All 32 of the shared lncRNAs were dysregulated in the same direction across both states: 20 were downregulated and 12 were upregulated, demonstrating complete directional fidelity and indicating a conserved expression signature irrespective of diabetes status (Figure 4C). Fold-change magnitudes were highly correlated between stages (Pearson r = 0.969, p < 0.0001; Figure 4D), with 78.1% of the shared lncRNAs showing greater absolute fold changes in type 2 diabetes than in insulin resistance (mean amplification factor: 1.16×). Key examples include SYBU-AS1 (−4.57 vs. −5.23), LINC01612 (−2.89 vs. −4.66), RORB-AS1 (−3.17 vs. −4.37), and FAM95A (−5.67 vs. −4.58). SYBU-AS1, LINC01612, and RORB-AS1 showed greater absolute fold changes in the Obese-T2D comparison, whereas FAM95A showed a smaller change (Figure 4E).

Together, these findings identify three categories of differential lncRNA expression: 96 lncRNAs meeting the significance criteria only in the Obese-IR versus lean comparison, 32 meeting the criteria in both comparisons with concordant directions of expression, and 376 meeting the criteria only in the Obese-T2D versus lean comparison. These patterns highlight both shared and comparison-specific expression differences in white adipose tissue across metabolic groups, without establishing temporal sequence or disease progression. Significance in only one comparison does not establish biological exclusivity.

IPA analysis of putative lncRNA cis-target genes highlights lipid metabolism, insulin signalling, and inflammatory pathways in the obese-IR versus lean comparison

IPA Core Analysis of the 196 protein-coding genes identified as putative cis-targets of the 128 lncRNAs differentially expressed in Obese-IR versus lean participants achieved 100% mapping to the QIAGEN Knowledge Base and identified 165 nominally enriched canonical pathways among the 687 tested (Fisher's exact test, p < 0.05; Figure 5A) [25]. The top-ranked pathways included lipid biosynthesis and fatty acid metabolism. Retinoate Biosynthesis I ($-\log_{10}p$ = 5.91) and Oleate Biosynthesis II ($-\log_{10}p$ = 5.79; gene overlap ratio = 0.31) were the most significantly enriched pathways, with contributing genes including CYB5A, FADS1, FADS2, and SCD. Fatty Acyl-CoA Biosynthesis ($-\log_{10}p$ = 5.22) and γ-Linolenate Biosynthesis II ($-\log_{10}p$ = 5.07) were also enriched; the latter was the only pathway meeting the threshold for predicted inhibition (activation z-score = −2.0). These results highlighted putative cis-target genes involved in fatty acid metabolism, including FADS1, FADS2, ELOVL3, ELOVL6, SCD, and ACSL1, without establishing their regulation by the associated lncRNAs [26, 27]. The enrichment of the Warburg Effect ($-\log_{10}p$ = 3.48) and HIF1α Signalling ($-\log_{10}p$ = 3.12) pathways highlighted processes related

10.3389/jpps.2026.17135

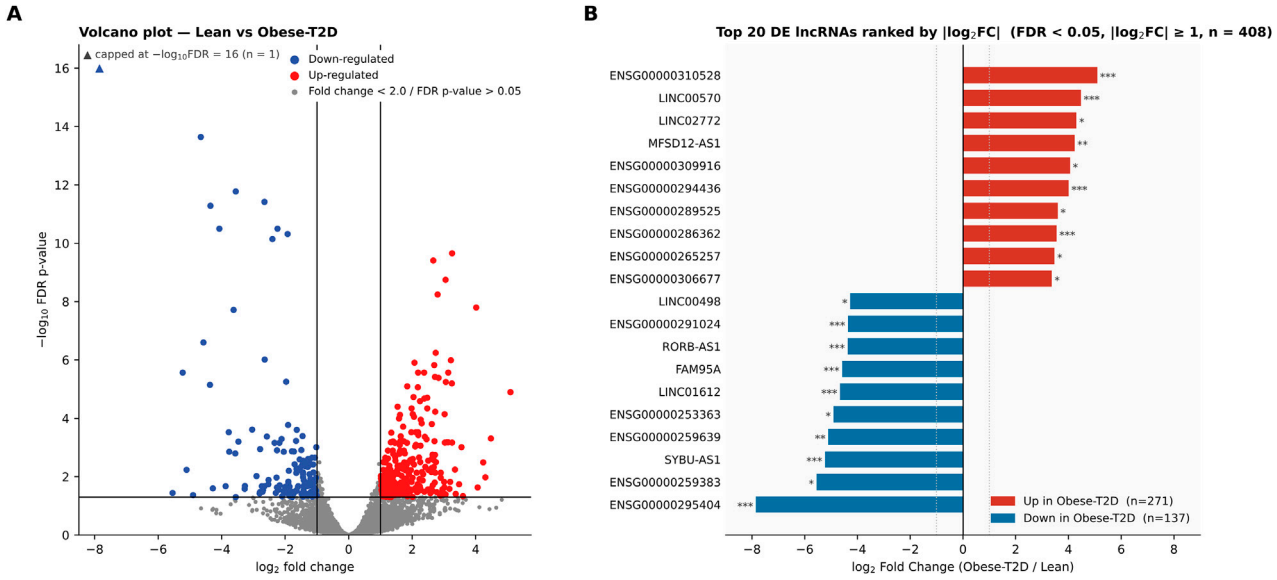


FIGURE 3
Differential lncRNA expression in white adipose tissue of obese type 2 diabetic versus lean subjects. **(A)** Volcano plot of 34,914 lncRNA features tested between lean (n = 8) and Obese-T2D (n = 8) groups. x-axis: $\log_2$ fold change (Obese-T2D/Lean); y-axis: $-\log_{10}$(FDR). Dashed vertical lines indicate $|\log_2 FC| = 1$; horizontal line indicates FDR = 0.05. Red: significantly upregulated; blue: significantly downregulated; grey: below threshold. **(B)** Top 20 DE lncRNAs by absolute $\log_2 FC$, comprising the 10 most upregulated and 10 most downregulated. Significance: *FDR < 0.05; **FDR < 0.01; ***FDR < 0.001.

to metabolic adaptation and hypoxia signalling. The Pathogen-Induced Cytokine Storm pathway was also enriched ($-\log_{10}p$ = 3.39) and met the threshold for predicted activation (activation z-score = 2.12), with contributing genes including CXCL1, CXCL8, HLA-DQA2, HLA-DRA, HLA-DRB1, SLC2A4, and TGFB2(3,21). Upstream regulator analysis identified the INSULIN family as a predicted inhibited regulator (activation z-score = −2.745; overlap p = 3.74×10^{-11}), associated with 27 input genes, including SLC2A4, GCK, PTEN, FADS1, FADS2, and IGF2. This prediction implicated insulin-responsive transcriptional processes among the putative cis-target genes but did not establish lncRNA-mediated impairment of insulin signalling.

Network analysis identified a PPARG-centred interaction network containing components associated with adipocyte biology (Figure 5B). The network included PPARG complexes, H3K4me1-modified nucleosomes, and the MLL4/MLL3-ASCOM complex, alongside lipid-metabolism genes such as FADS1, FADS2, SCD, CYB5A, and ACSL1. Connections involving the PPARG:RXRA/SMRT corepressor complexes provided a possible transcriptional context for these genes, without demonstrating altered chromatin regulation or PPARG-mediated silencing in the study samples [28]. AZGP1, a gene associated with lipid mobilisation, also appeared in the PPARG-centred network. Its inclusion suggested a potential connection to lipid-handling processes relevant to the elevated free fatty acid phenotype reported in the source cohort, although a direct association was not established in this analysis [29]. Together, these pathway and network analyses highlighted the importance of lipid metabolism, insulin-responsive processes, inflammatory signalling, and PPARG-associated adipocyte biology among the putative cis-target genes of lncRNAs differentially expressed in Obese-IR versus lean participants. These findings generate hypotheses for functional investigation.

T2D lncRNA cis-target IPA analysis reveals stage-specific pathway expansion superimposed on a conserved lipid-epigenetic core

IPA Core Analysis of 88 protein-coding cis-target genes of 408 T2D-stage DE lncRNAs identified 122 significant canonical pathways from 527 tested (Figure 6). Of these, 55 were also significant in the IR-stage analysis, indicating overlapping enriched pathways between the two analyses, while 67 were exclusive to type 2 diabetes and were enriched only in the Obese-T2D analysis.

The smaller cis-target gene set at the T2D stage (88 genes vs. 196 genes at the IR stage) is discussed in Materials and Methods 2.4. The 100% IPA mapping rate for both gene sets reflects annotation coverage and does not validate the lncRNA–target relationships.

The most significantly enriched pathway was Fatty Acyl-CoA Biosynthesis ($-\log_{10}$ p = 6.91, ratio = 0.135, z = −2.236), driven by ACSL1, ELOVL3, ELOVL6, FASN, and SCD. This pathway reached predicted inhibition significance in type 2 diabetes (z = −2.236) compared with only trending inhibition in insulin resistance (z = −1.342), indicating a difference in the predicted state of fatty acid activation and elongation between the groups [26, 27]. Among the conserved, shared pathways, Ethanol Degradation II ($-\log_{10}$ p = 5.26), Noradrenaline and Adrenaline Degradation ($-\log_{10}$ p = 5.12), Retinoate Biosynthesis I ($-\log_{10}$ p = 3.27), Oleate Biosynthesis II

10.3389/jpps.2026.17135

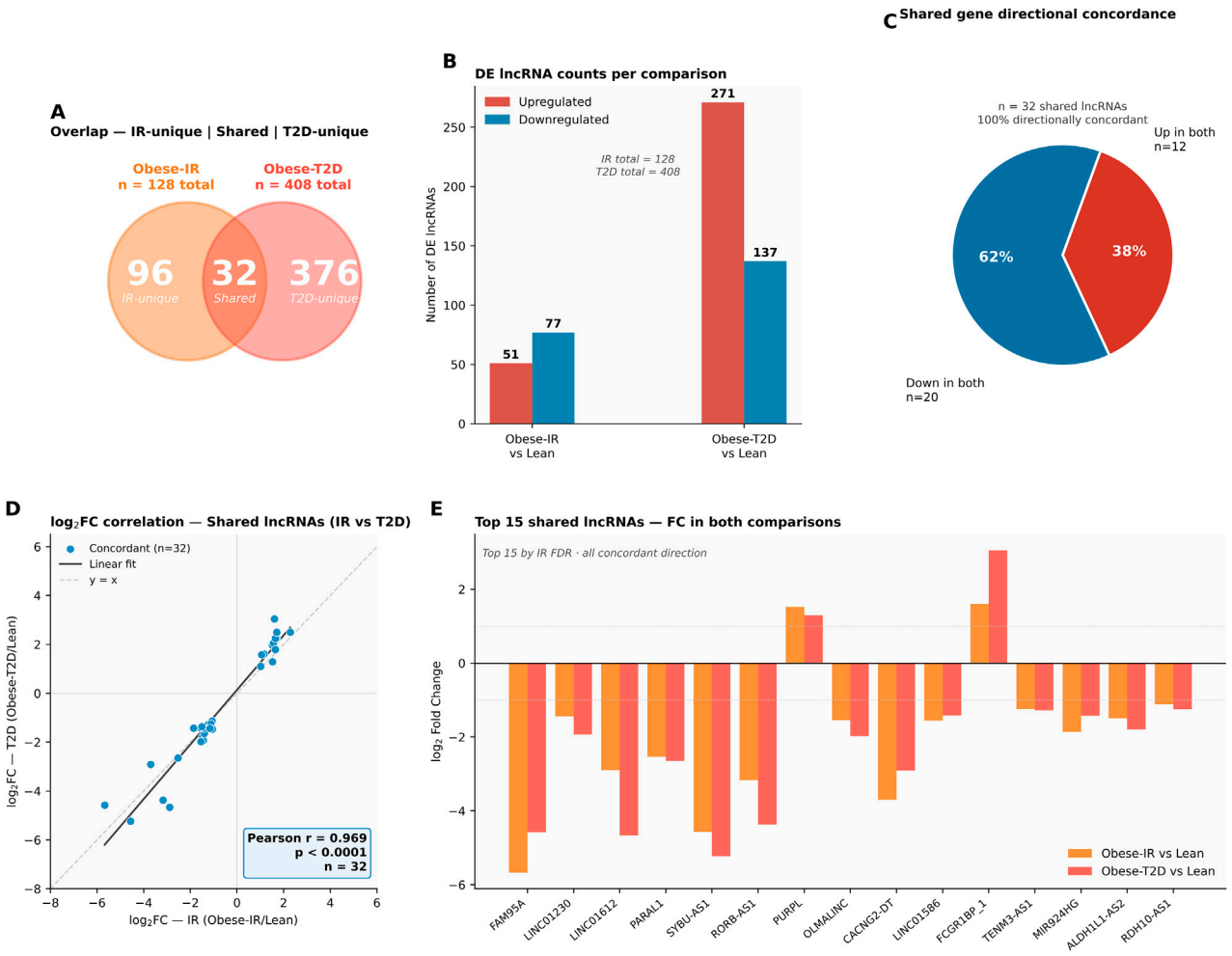


FIGURE 4
Overlap analysis identifies shared and comparison-specific differentially expressed lncRNAs in human white adipose tissue across metabolic groups. **(A)** Venn diagram of differentially expressed (DE) lncRNAs in the Obese-IR versus lean (n = 128) and Obese-T2D versus lean (n = 408) comparisons (FDR <0.05, $|\log_2 FC| \geq 1$), showing 96 lncRNAs significant only in the Obese-IR comparison, 32 shared between comparisons, and 376 significant only in the Obese-T2D comparison. **(B)** Grouped bar chart showing the numbers of upregulated and downregulated DE lncRNAs in each comparison. **(C)** Pie chart showing directional concordance among the 32 shared lncRNAs: all showed the same direction of differential expression in both comparisons, with 20 downregulated and 12 upregulated. **(D)** Scatter plot comparing $\log_2 FC$ values for the 32 shared lncRNAs between the Obese-IR versus lean and Obese-T2D versus lean comparisons (Pearson r = 0.969, $p < 0.0001$). The dashed line indicates equal $\log_2 FC$ values (y = x). **(E)** Grouped bar chart comparing $\log_2 FC$ values for the top 15 shared lncRNAs, ranked by ascending FDR-adjusted p-value in the Obese-IR versus lean comparison. Positive and negative $\log_2 FC$ values indicate higher and lower expression, respectively, relative to lean controls. Significance in only one comparison does not establish biological exclusivity or temporal progression.

($-\log_{10}$ p = 3.11), and Epigenetic Regulation by MLL3/MLL4 Complexes ($-\log_{10}$ p = 3.04) suggested that aldehyde dehydrogenase-related, retinoid-PPAR-related and PPARG-associated chromatin-remodelling pathways, highlighted among the Obese-IR cis-target genes (Section *Ingenuity pathway analysis*), were also enriched among the Obese-T2D cis-target genes [30].

The two T2D-unique pathways within the top 20 were Triacylglycerol Biosynthesis ($-\log_{10}$ p = 3.00) and Stearate Biosynthesis I ($-\log_{10}$ p = 2.82), both relating to lipogenesis and enriched only in the Obese-T2D analysis [30]. Of the 67 T2D-exclusive pathways, LPS/IL-1 Mediated Inhibition of RXR Function ($-\log_{10}$ p = 2.56), NAFLD Signalling ($-\log_{10}$ p = 2.23), and Granulocyte Adhesion and Diapedesis ($-\log_{10}$ p = 2.36) were notable; they relate to endotoxin-associated RXR signalling, hepatic lipid signalling, and neutrophil trafficking and were enriched only among the Obese-T2D cis-target genes [31–33].

Hierarchical co-expression clustering of differentially expressed lncRNAs

Following identifier harmonisation and expression filtering, 127 of the 128 lncRNAs differentially expressed in the Obese-IR versus lean comparison were included in hierarchical co-expression clustering (Figure 7). ENSG00000176868 was excluded because it was detected at a raw count ≥1 in only three of the 24 samples, which is below the minimum requirement of five samples.

The dendrogram was partitioned into five clusters containing 4, 50, 2, 70, and 1 lncRNAs, respectively. The cluster assignments of the

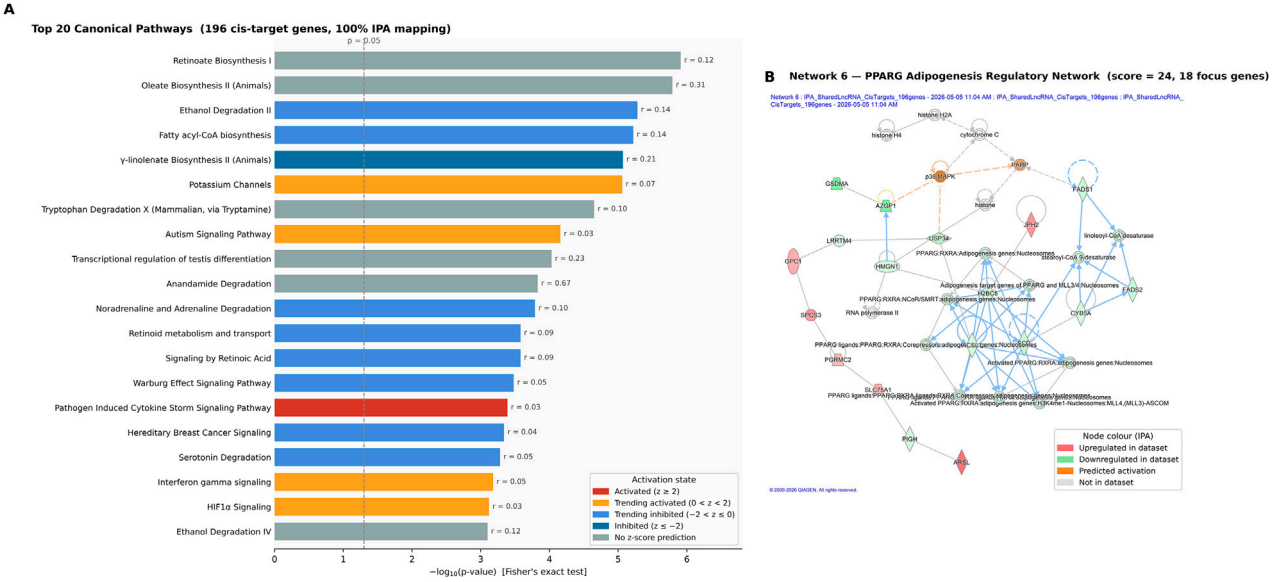


FIGURE 5
IPA Core Analysis of protein-coding cis-target genes of 128 IR-stage DE lncRNAs in hyperinsulinaemic insulin-resistant white adipose tissue. Cis-target genes were identified within ±500 kb of each DE lncRNA using GENCODE v44 coordinates. **(A)** Top 20 enriched canonical pathways ranked by $-\log_{10}$(p-value; Fisher's exact test). Bar colour: red = activated ($z \geq 2$); orange = trending activated; light blue = trending inhibited; blue = inhibited ($z \leq -2$); grey = no prediction. Gene overlap ratio (r) shown at bar ends. **(B)** IPA Network 6 (score = 24, 18 focus molecules), highest-scoring adipose-relevant network, centred on PPARG-driven adipogenesis regulation. Node colour: red = upregulated; green = downregulated; orange = predicted activated; grey = not in dataset. Edges: blue = predicted activation; dashed orange = indirect interaction. Node shape: diamond = enzyme; ellipse = complex; pentagon = transporter.

candidate lncRNAs FAM95A, LINC01230, PARAL1, LINC01612, SYBU-AS1 and RORB-AS1 are given in the Supplementary Data Sheet 1, sheet Cluster_assignments. These modules describe similarities in lncRNA expression profiles across the analysed samples and do not establish functional interactions or associations with individual clinical traits. Complete module assignments are provided in the Supplementary Data Sheet 1, sheet DE_lncRNAs.

FAM95A and LINC01230 show exploratory discriminatory performance for hyperinsulinaemic insulin resistance

To evaluate the translational potential of the top IR-stage DE lncRNAs as tissue biomarkers of hyperinsulinaemic insulin resistance, we performed ROC analysis using $\log_2$(CPM+1) expression values across all 24 subjects. AUCs are reported with 95% confidence intervals, which were calculated using the DeLong method and truncated at 1.000.

FAM95A was the strongest discriminator of lean from obese participants with hyperinsulinaemic insulin resistance without diagnosed diabetes (Obese-IR), achieving an AUC = 0.867 (95% CI 0.675–1.000; Figure 8A) above the 0.80 threshold for good biomarker performance. LINC01230 demonstrated comparable performance (AUC = 0.828, 95% CI 0.593–1.000) for the same comparison (Figures 8A,C), with both point estimates exceeding the 0.70 threshold for acceptable performance and both intervals lying above the random classifier value of 0.5; the lower confidence limits (0.675 and 0.593) indicate that precision is limited with eight participants per group.

Stage-specific analysis of FAM95A revealed consistent discriminatory capacity across the metabolic continuum: AUC = 0.867 (95% CI 0.675–1.000) for Lean vs. Obese-T2D and AUC = 0.539 (95% CI 0.273–0.805) for Obese-IR vs. Obese-T2D (Figure 8B), indicating that FAM95A expression distinguishes between metabolically healthy and obese dysfunctional states, but does not track glycaemic decompensation specifically. In contrast, LINC01230 showed higher AUCs in comparisons involving the Obese-T2D group (AUC = 0.828, 95% CI 0.593–1.000, for Lean vs. Obese-IR; AUC = 0.844, 95% CI 0.597–1.000, for Obese-IR vs. Obese-T2D; and AUC = 0.969, 95% CI 0.896–1.000, for Lean vs. Obese-T2D; Figures 8B,C), consistent with a greater expression difference in the Obese-T2D group. Together, FAM95A and LINC01230 represent candidate tissue biomarkers of adipose insulin resistance in participants without diagnosed diabetes whose diagnostic performance in independent, well-phenotyped cohorts warrants further investigation.

lncRNA–mRNA cis-regulatory interaction network reveals coordinated targeting of lipid biosynthesis, insulin signalling, and immune activation programmes in insulin-resistant adipose tissue

To visualise the regulatory architecture connecting IR-stage DE lncRNAs to their functional cis-target programmes, we

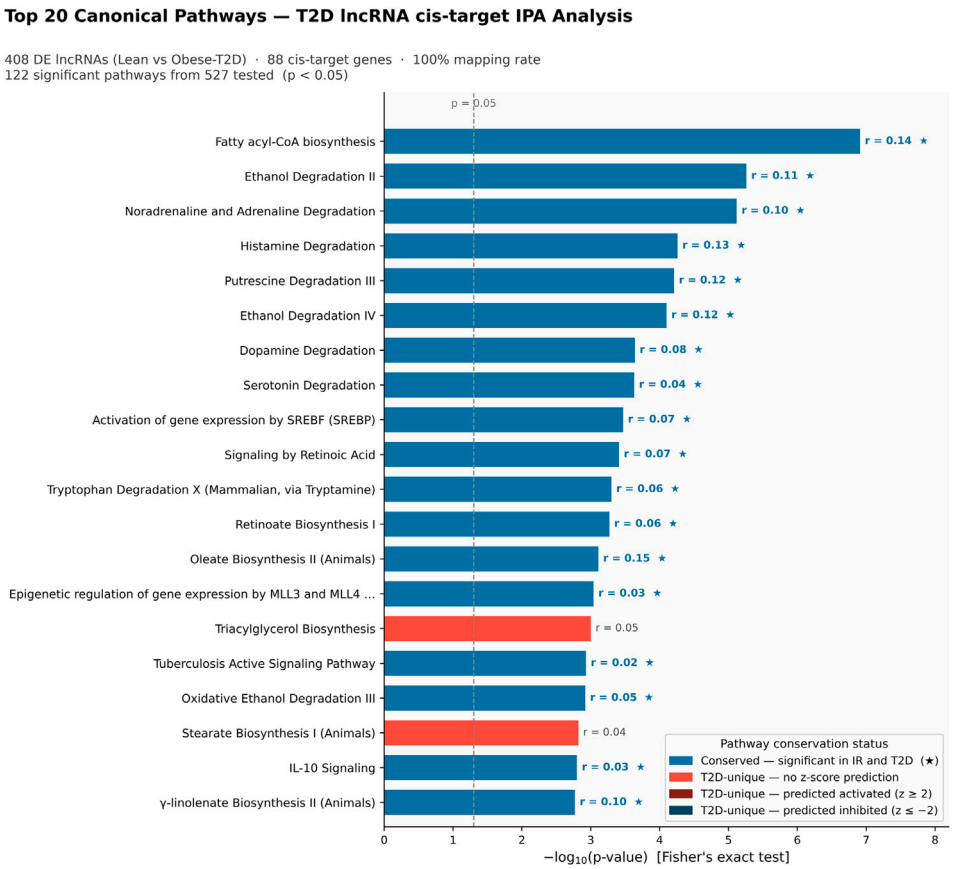


FIGURE 6
IPA canonical pathway analysis of protein-coding cis-target genes of differentially expressed lncRNAs in type 2 diabetic WAT. Core Analysis was performed on cis-target protein-coding genes of 408 lncRNAs significantly DE in the Lean vs. Obese-T2D comparison. The top 20 enriched canonical pathways are ranked by $-\log_{10}$(p-value; Fisher's exact test) from 122 significant pathways across 527 tested pathways. Blue bars (★) indicate pathways also significant in the IR analysis (conserved across disease stages). Red bars indicate pathways exclusive to T2D. Bar shading reflects predicted activation z-score where available (dark red = activated $z \geq 2$; dark blue = inhibited $z \leq -2$). Gene overlap ratio (r) is shown at bar ends. Dashed vertical line marks p = 0.05.

constructed a three-layer lncRNA–mRNA cis-regulatory interaction network (Figure 9). Six top IR-stage DE lncRNAs were connected to 196 IPA-validated cis-target protein-coding genes (±500 kb, GENCODE v44) through four IPA pathway hubs: Lipid Biosynthesis, Insulin Signalling, Immune/Cytokine, and PPARG/Chromatin regulation. FAM95A and PARAL1 connected predominantly to PPARG/Chromatin and Lipid Biosynthesis cis-targets, including AZGP1, MTTP, SCD, FADS1, and FADS2, which are all downregulated in insulin-resistant adipose tissue. LINC01612 and RORB-AS1 showed connections to Immune/Cytokine pathway cis-targets including CXCL1 ($\log_2$FC = 2.1), CXCL8 ($\log_2$FC = 1.9), and TGFB2 ($\log_2$FC = +1.4), consistent with the innate immune activation identified in the IPA upstream regulator analysis. SYBU-AS1 and LINC01230 connected to Insulin Signalling cis-targets including SLC2A4, GCK, and PTEN, relating to the predicted inhibition of the INSULIN family upstream regulator ($z = -2.745$, $p = 3.74 \times 10^{-11}$). This network visualisation summarises the putative cis-target relationships of six selected IR-stage DE lncRNAs; genomic proximity does not establish regulatory interaction.

Discussion

This study provides a genome-wide characterisation of lncRNA expression differences between lean participants, obese participants with hyperinsulinaemic insulin resistance without diagnosed diabetes, and obese participants with type 2 diabetes in human white adipose tissue. Using the MD-Lipolysis cohort [16], which uniquely integrates deep metabolic phenotyping including OGTT, HOMA-IR, the Matsuda index, microdialysis, and adipose biopsy with adipose tissue RNA sequencing, we identified 128 differentially expressed lncRNAs in the Obese-IR group, 408 in the Obese-T2D group, and a 32-lncRNA overlap with concordant direction in both comparisons. Pathway and network analysis of their protein-coding cis-target genes highlighted PPARG-associated adipogenesis, predicted inhibition of fatty acid desaturation and elongation pathways, insulin-signalling-related genes, and comparison-specific inflammatory and lipogenic pathways among the putative cis-target genes. These are hypothesis-generating observations in participants without diagnosed diabetes.

PERMANOVA detected a difference between lean and Obese-IR participants ($p = 0.0002$), whereas the lean versus Obese-T2D comparison was not statistically significant ($p = 0.176$). This does not establish equivalence between lean and Obese-T2D participants or

10.3389/jpps.2026.17135

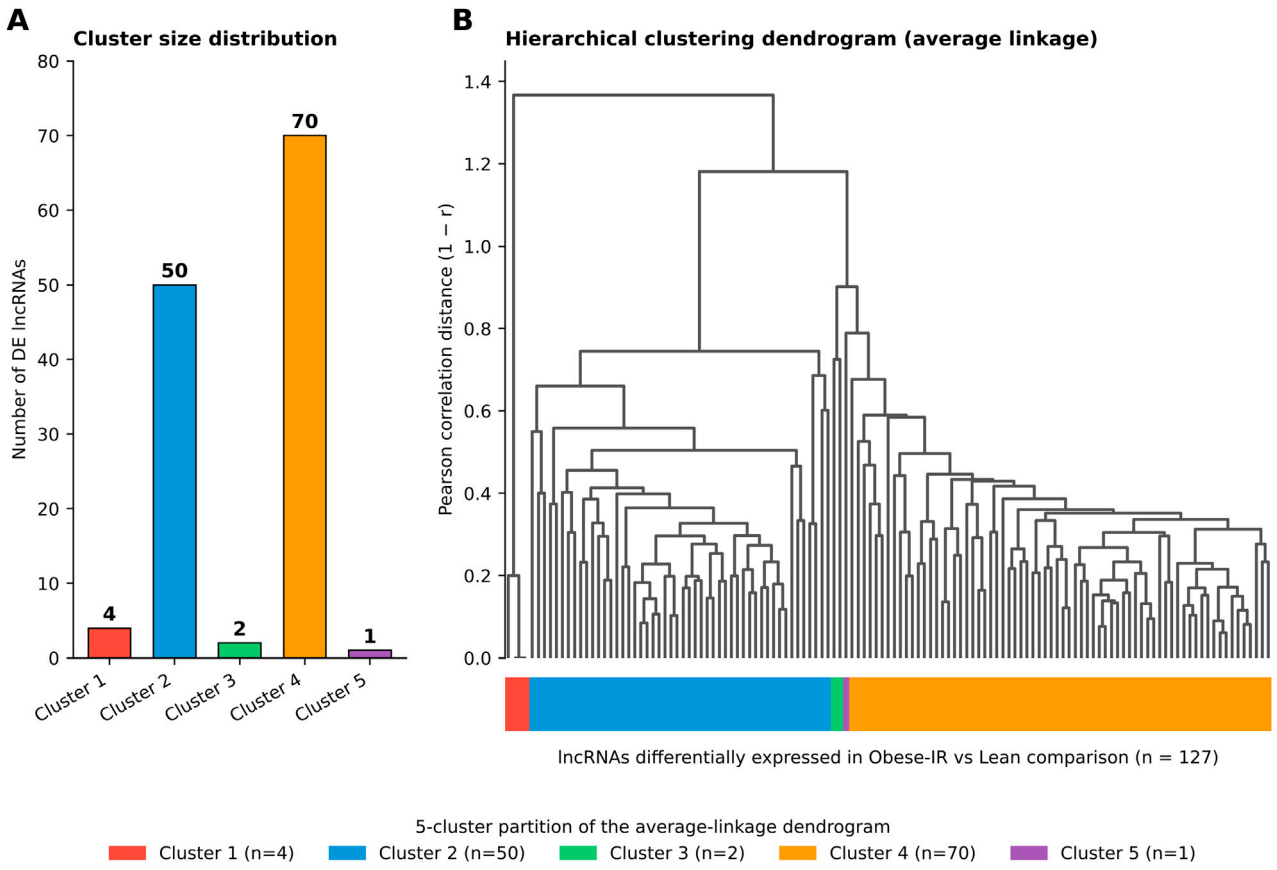


FIGURE 7
Hierarchical co-expression clustering of lncRNAs differentially expressed in the Obese-IR versus lean comparison. The analysis included 127 lncRNAs, meeting the detection threshold of raw count ≥1 in at least five of the 24 samples. ENSG00000176868 was excluded because it was detected in three samples. Clustering used $\log_2$(CPM + 1) expression profiles across all 24 participants, Pearson correlation distance (1 – r), and average linkage. The dendrogram was partitioned into five clusters. **(A)** Cluster-size distribution, with counts shown above each bar. Clusters 1–5 contained 4, 50, 2, 70, and 1 lncRNAs, respectively. **(B)** Hierarchical clustering dendrogram. Each terminal leaf represents one lncRNA, and the colour strip indicates cluster membership in dendrogram leaf order. Colours correspond to those in **(A)**. The five-cluster partition is descriptive and does not imply five independently validated biological modules.

a greater biological effect in Obese-IR. Within-group variability and the small sample size may contribute, although these explanations require further assessment. The first two principal components capture only 27.0% of expression variance, so visual separation should not be equated with statistical significance. These findings do not establish a temporal peak or reversal of lncRNA dysregulation.

Spatial transcriptomics has identified human adipocyte subpopulations with distinct sensitivities to insulin [15], providing context for investigating adipose expression differences across metabolic groups.

The predominance of downregulated lncRNAs at the insulin-resistant stage (77 downregulated vs. 51 upregulated), followed by directional reversal at the type 2 diabetic stage (271 upregulated vs. 137 downregulated), mirrors patterns observed in post-bariatric surgery lncRNA studies where transcriptional repression-to-activation shifts accompany changes in metabolic state [34]. These patterns could reflect different expression programmes in the Obese-IR and Obese-T2D groups, for example repression-dominant versus activation-dominant profiles involving stress-response, immune and lipogenic genes; evidence that the lncRNA LINK-A promotes HIF-1α-mediated adipose inflammatory remodelling in mice fed a high-fat diet [35] is compatible with this possibility. Chromatin state and corepressor engagement were not measured here, so this interpretation remains speculative.

The 32 lncRNAs dysregulated with 100% directional concordance across both states, with strongly correlated $\log_2$ fold changes (Pearson r = 0.969, $p < 0.0001$; mean absolute fold-change ratio 1.16×), constitute a conserved adipose metabolic stress signature. Strikingly, none of the top conserved candidates FAM95A, SYBU-AS1, LINC01612, or RORB-AS1 have published functional characterisation in adipose tissue. FAM95A was the most significantly downregulated ($\log_2$FC = −5.67, FDR = 3.11×10^{-9} in insulin resistance; $\log_2$FC = −4.58 in type 2 diabetes) and maps within 500 kb of TRIM55, an E3 ubiquitin ligase implicated in metabolic stress responses. SYBU-AS1, LINC01612, and RORB-AS1 similarly showed suppression with greater effect sizes in the Obese-T2D comparison, which may warrant testing for roles in adipocyte transcriptional identity. The directional concordance of this conserved core parallels linc-GALNTL6-4, whose expression has been reported to track adipose dysfunction and to normalise upon weight loss [9]; whether the 32-lncRNA core is reversible or

10.3389/jpps.2026.17135

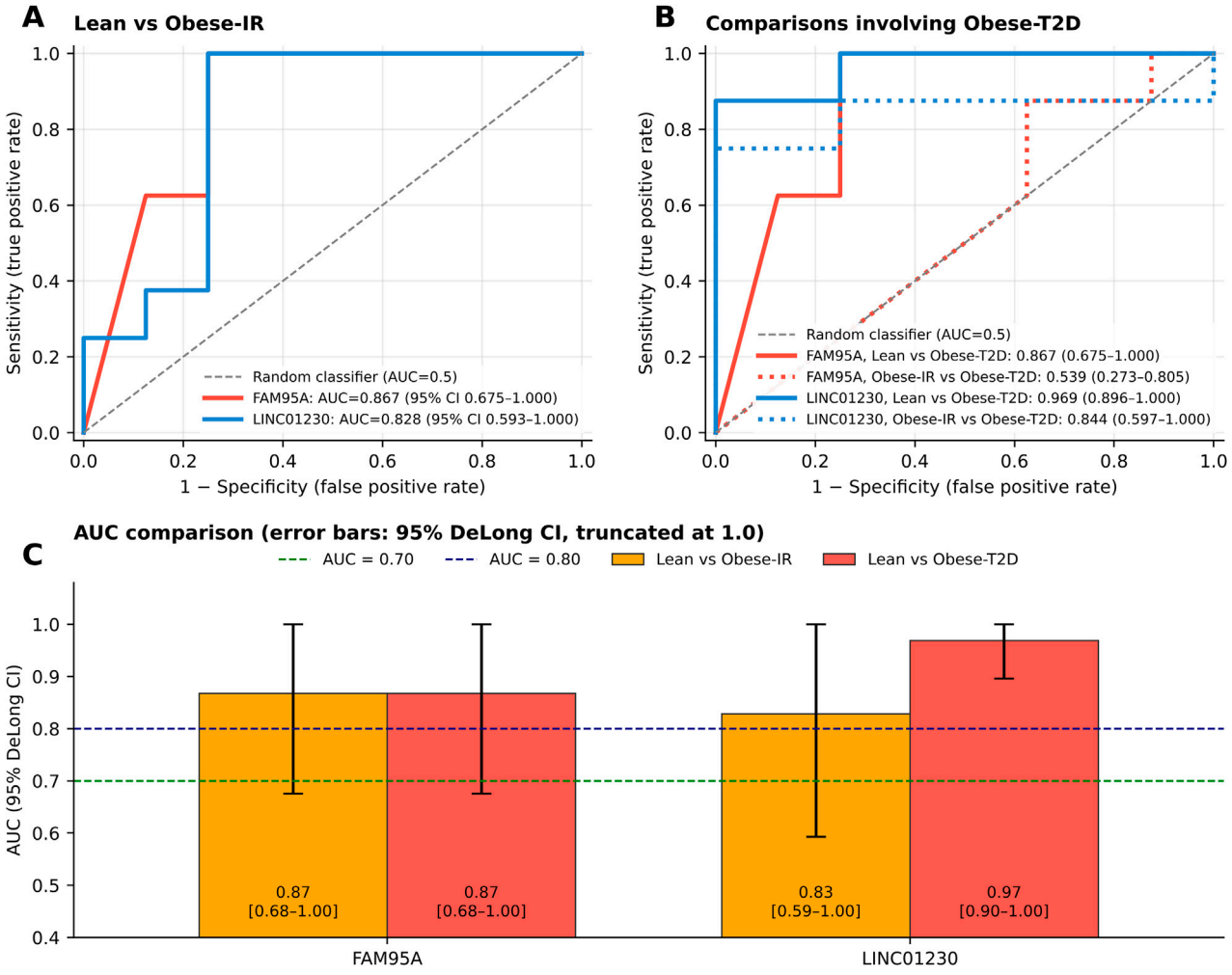


FIGURE 8
ROC analysis shows exploratory discriminatory performance of FAM95A and LINC01230 for hyperinsulinaemic insulin resistance across the three groups. ROC analysis was performed using $\log_2$(CPM+1) expression values across all 24 subjects (n = 8 per group). **(A)** ROC curves for FAM95A (AUC = 0.867, 95% CI 0.675–1.000) and LINC01230 (AUC = 0.828, 95% CI 0.593–1.000) discriminating lean healthy from obese participants with hyperinsulinaemic insulin resistance without diagnosed diabetes (Obese-IR). The dashed diagonal line represents a random classifier (AUC = 0.5). **(B)** Stage-specific ROC curves for FAM95A and LINC01230 across Lean vs. Obese-T2D and Obese-IR vs. Obese-T2D comparisons. AUCs (95% CI) – FAM95A: Lean vs. Obese-T2D 0.867 (0.675–1.000), Obese-IR vs. Obese-T2D 0.539 (0.273–0.805); LINC01230: Lean vs. Obese-T2D 0.969 (0.896–1.000), Obese-IR vs. Obese-T2D 0.844 (0.597–1.000). **(C)** Grouped bar chart of AUC values for both lncRNAs across Lean vs. Obese-IR (orange) and Lean vs. Obese-T2D (red) comparisons (error bars show 95% DeLong confidence intervals). Dashed lines indicate AUC thresholds of 0.70 (acceptable) and 0.80 (good) biomarker performance. AUC: area under the curve; ROC: receiver operating characteristic; CPM: counts per million. Confidence intervals were calculated by the DeLong method and truncated at 1.000.

therapeutically accessible remains to be tested through gain- and loss-of-function studies in primary human adipocytes.

Hierarchical clustering provided an exploratory description of expression similarities among the 127 retained lncRNAs. The five-cluster partition was dominated by two clusters containing 50 and 70 transcripts, with the remaining clusters containing four, two, and one transcript, respectively. Associations with individual metabolic traits were not assessed.

IPA Network 6 centred on a PPARG:RXRA complex associated with H3K4me1-modified adipogenesis target genes via the MLL4/MLL3-ASCOM chromatin remodelling complex, which is the primary molecular switch controlling adipogenic competence [28]. The presence of lncRNA cis-target genes within this network node is consistent with, but does not demonstrate, a role for these lncRNAs in PPARG-associated adipogenic regulation. This is compatible with recently characterised PPARG/lncRNA axes: lncRNA Lexis operates through PPARG to suppress thermogenic programmes, and its adipose-specific deletion improves insulin sensitivity and counteracts diet-induced obesity in mice [36]; similarly, ADIPINT regulates lipid synthesis through pyruvate carboxylase interaction, with its expression linked to adipose insulin resistance in human white adipose tissue [37]. Whether FAM95A, SYBU-AS1, or LINC01612 operate through analogous mechanisms chromatin scaffolding of PPARG:RXRA, modulation of MLL4/MLL3-ASCOM, or NCoR/SMRT corepressor binding requires dedicated functional validation. Parallel human adipose evidence from linc-

10.3389/jpps.2026.17135

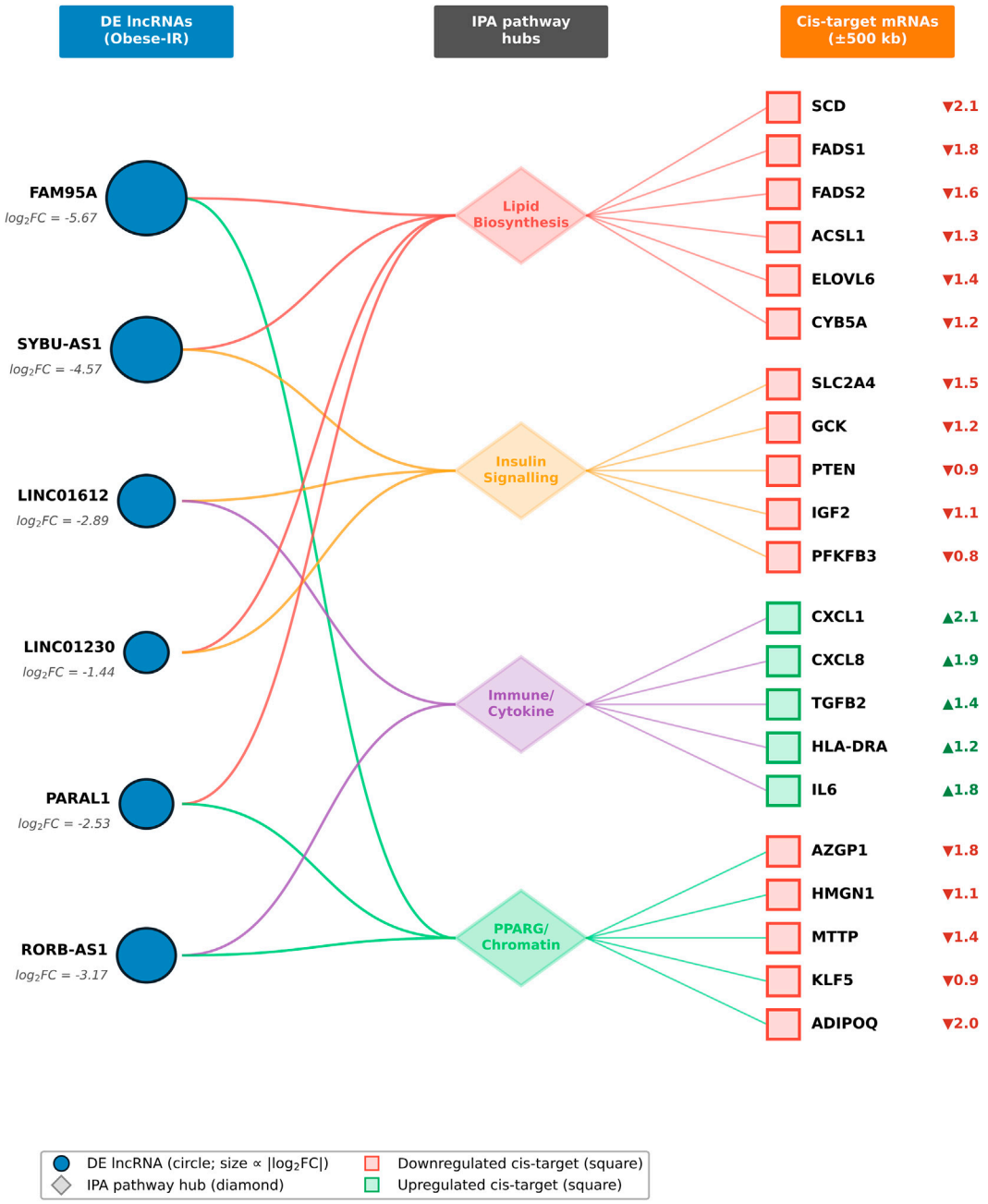


FIGURE 9
lncRNA–mRNA cis-regulatory interaction network in hyperinsulinaemic insulin-resistant white adipose tissue. Three-layer network connecting IR-stage DE lncRNAs (left; blue circles) to IPA-enriched pathway hubs (centre; diamonds) and cis-target protein-coding mRNAs (right; squares) identified within ±500 kb using GENCODE v44 coordinates. Node size for lncRNAs reflects absolute log_2FC magnitude. Arrows indicate cis-regulatory connections between lncRNAs and pathway hubs; lines connect pathway hubs to individual cis-target mRNAs. Square node colour indicates IPA pathway membership: red = Lipid Biosynthesis; orange = Insulin Signalling; purple = Immune/Cytokine; green = PPARG/Chromatin. ▼ and ▲ symbols indicate downregulated and upregulated cis-target mRNAs, respectively, with absolute log_2FC shown. Dashed vertical lines demarcate the three network layers.

ADAIN [10] and ADIPINT [37] demonstrates that individual adipose lncRNAs can have direct and measurable consequences for adipocyte identity and lipid metabolism, providing biological context for the hypotheses generated here. The lncRNA–mRNA proximity network (Figure 9) illustrates these putative relationships at the level of genomic proximity, without establishing regulation. FAM95A and PARAL1 are connected to PPARG/Chromatin and Lipid Biosynthesis cis-targets, including AZGP1, SCD, FADS1, and FADS2; LINC01612 and RORB-AS1 to Immune/Cytokine targets including CXCL1 (log_2FC = 2.1) and TGFB2 (log_2FC = 1.4); and SYBU-AS1 and LINC01230 are connected to Insulin Signalling targets, including SLC2A4, GCK, and PTEN relating to the predicted inhibition of the INSULIN family upstream regulator ($z = -2.745$, $p = 3.74 \times 10^{-11}$) only at the level of

genomic proximity. AZGP1 appears as a node in the PPARG-centred network, which may be related to the elevated free fatty acid phenotype reported in the source cohort, although a direct association was not tested [16, 29].

The top-ranked canonical pathways in both analyses, Retinoate Biosynthesis I, Oleate Biosynthesis II, Fatty Acyl-CoA Biosynthesis, and γ-Linolenate Biosynthesis II, suggest the involvement of lipid-remodelling-related genes in both comparisons. The Fatty Acyl-CoA Biosynthesis pathway uniquely reached predicted inhibition significance in type 2 diabetes ($z = -2.236$ vs. $z = -1.342$ in insulin resistance), consistent with a difference in the predicted state of fatty acid desaturation and elongation between the groups. FADS1, FADS2, SCD, ELOVL3, ELOVL6, and ACSL1 appeared consistently as lncRNA cis-targets across both stages; their dysregulation is associated with altered membrane phospholipid composition and increased type 2 diabetes risk [26, 27] and with impaired adipose lipid storage [30, 38] raising the hypothesis that lncRNA cis-regulation may contribute to adipose lipid remodelling; direct regulatory relationships require experimental confirmation.

Upstream regulator analysis identified INSULIN family signalling as the most significantly predicted inhibited regulator ($z = -2.745$, $p = 3.74 \times 10^{-11}$; 27 cis-target genes including SLC2A4, GCK, PTEN, and FADS1/2). This prediction is derived from lncRNA fold changes assigned to neighbouring genes and does not establish functional coupling between lncRNA changes and insulin effector expression, nor a mechanism for hyperinsulinaemic insulin resistance. The concurrent enrichment of the HIF-1α Signalling and Warburg Effect pathways is consistent with adipose tissue hypoxia in obesity driving macrophage polarisation, preadipocyte differentiation failure, and extracellular matrix fibrosis [31]. At the type 2 diabetic stage, LPS/IL-1 Mediated Inhibition of RXR Function adds an endotoxin-related signalling pathway to the corepressor-related context highlighted in the Obese-IR network, a possible additional pathway relating to PPARG:RXRA signalling that was enriched only in the Obese-T2D analysis. T2D-exclusive NAFLD Signalling is consistent with lncRNA H19-mediated hepatic lipid dysregulation [33], a possible cross-tissue parallel that was not tested here, while Granulocyte Adhesion and Diapedesis is consistent with immune-cell infiltration reported in diabetic adipose tissue [3].

ROC analysis established FAM95A (AUC = 0.867, 95% CI 0.675–1.000) and LINC01230 (AUC = 0.828, 95% CI 0.593–1.000) as candidate tissue biomarkers for discriminating lean from obese participants with hyperinsulinaemic insulin resistance without diagnosed diabetes, with both point estimates exceeding the 0.80 threshold for good biomarker performance (the wide intervals reflect the small sample). FAM95A maintained equivalent discriminatory capacity for lean versus type 2 diabetic discrimination (AUC = 0.867, 95% CI 0.675–1.000) but showed poor IR-to-T2D discrimination (AUC = 0.539, 95% CI 0.273–0.805), indicating that it separates both obese groups from lean participants but not the two obese groups from each other. In contrast, LINC01230 showed higher AUCs in comparisons involving the Obese-T2D group (AUC = 0.828, 95% CI 0.593–1.000, for Lean vs. Obese-IR; AUC = 0.844, 95% CI 0.597–1.000, for Obese-IR vs. Obese-T2D; and AUC = 0.969, 95% CI 0.896–1.000, for Lean vs. Obese-T2D), consistent with a greater expression difference in the Obese-T2D group.

One strength of this study is the selection of obese participants based on fasting hyperinsulinaemia despite relatively preserved glycaemic control at the group level, together with deep metabolic phenotyping including OGTT, HOMA-IR, the Matsuda index, microdialysis, and adipose biopsy [16]. Genomic proximity was used to nominate putative cis-target genes as a basis for exploratory functional interpretation [5, 6]. Together, the shared and comparison-specific lncRNA expression patterns identify candidates for further investigation of adipose biology in hyperinsulinaemic insulin resistance and type 2 diabetes.

Limitations

Several limitations should be considered when interpreting these findings. First, the small sample size (eight participants per group) limits statistical power, particularly with regard to detecting transcripts with modest expression differences, and reduces the precision and generalisability of the estimates. Second, the cross-sectional comparison of independent participant groups precludes conclusions regarding temporal progression or causality. Insulin resistance was characterised using fasting insulin and HOMA-IR rather than being directly measured by a hyperinsulinaemic–euglycaemic clamp. Furthermore, the absence of an obese insulin-sensitive comparison group prevents the separation of adiposity-related effects from those associated with insulin resistance. Third, bulk RNA sequencing of subcutaneous adipose tissue captures a mixture of adipocytes, stromal-vascular cells and immune cells; therefore, the observed expression differences may reflect changes in cellular composition, gene expression within individual cell types, or both. Single-cell or spatial approaches are needed to distinguish between these contributions.

The computational nature of this study also limits mechanistic interpretation. Putative cis-target genes were nominated by genomic proximity within ±500 kb, which does not establish regulatory interactions, and sensitivity analyses using narrower windows were not performed. Moreover, lncRNA fold changes and FDR values assigned to neighbouring protein-coding genes for IPA do not represent measured expression changes in those genes. Consequently, the resulting directional pathway and upstream regulator predictions cannot establish target-gene activation or inhibition. Experimental perturbation of candidate lncRNAs in primary human adipocytes is required to determine their biological functions and potential effects on neighbouring genes. Finally, the ROC analyses were conducted in the discovery dataset without independent validation, introducing a risk of optimistic AUC estimates. Independent cohorts and longitudinal studies are therefore required to establish reproducibility, predictive value, and clinical relevance.

Conclusion

In this cross-sectional study, we identified shared and comparison-specific lncRNA expression patterns in human white adipose tissue: in total, 96 lncRNAs met the differential expression criteria only in the Obese-IR versus lean comparison, 32 met the criteria in both comparisons with concordant directions of expression, and 376 met the criteria only in the Obese-T2D versus lean comparison. Pathway and network analyses suggested potential links to PPARG-associated adipogenesis and fatty acid

metabolism. FAM95A and LINC01230 showed exploratory potential for distinguishing lean from hyperinsulinaemic insulin-resistant participants without diagnosed diabetes, while co-expression analysis identified clusters of lncRNAs with similar expression patterns. These findings highlight lncRNA expression differences present in adipose tissue from hyperinsulinaemic insulin-resistant participants without diagnosed diabetes, and nominate candidates for independent validation and functional investigation. Longitudinal studies and functional experiments are needed to establish temporal relationships, predictive value, causal regulatory roles, and potential therapeutic relevance.

Data availability statement

Publicly available datasets were analysed in this study. The RNA sequencing data are available in the NCBI Gene Expression Omnibus under accession GSE141432, and raw reads in the Sequence Read Archive under accession SRP234695. Analysis code is available from the corresponding author upon reasonable request.

Author contributions

Conceptualization: KE and AH; Data curation: KE; Formal analysis: KE; Investigation: KE, AH, and AA; Methodology: KE; Writing original draft: KE; Writing review and editing: KE, AH, and AA; Supervision: AH and AA. All authors contributed to the article and approved the submitted version.

Funding

The author(s) declared that financial support was received for this work and/or its publication. This study was supported by funding from the Al Saqer Group (grant number 19301000) and the Research Office at Abu Dhabi University, which are gratefully acknowledged.

Acknowledgments

The authors gratefully acknowledge the MD-Lipolysis study participants and the original investigators (Fryk et al., EBioMedicine 2021) for making the RNA-seq data publicly available via the NCBI Gene Expression Omnibus under accession number GSE141432.

Conflict of interest

The author(s) declared that this work was conducted in the absence of any commercial or financial relationships that could be construed as a potential conflict of interest.

Generative AI statement

The author(s) declared that generative AI was not used in the creation of this manuscript.

Any alternative text (alt text) provided alongside figures in this article has been generated by Frontiers with the support of artificial intelligence and reasonable efforts have been made to ensure accuracy, including review by the authors wherever possible. If you identify any issues, please contact us.

Supplementary material

The Supplementary Material for this article can be found online at: https://www.frontierspartnerships.org/articles/10.3389/jpps.2026.17135/full#supplementary-material

References

1. IDF diabetes atlas 2025. *Diabetes Atlas*. (2026) Available online at: https://diabetesatlas.org/resources/idf-diabetes-atlas-2025/(Accessed May 9, 2026)

2. Zhang G, Mei H, Sheng Q, Chen Y, Zhang X, Diwon A, et al. Global burden of type 2 diabetes attributable to behavioral risks: insights and projections to 2050 based on the global burden of disease study 2021. *Int J Public Health* (2026) 71:1608765. doi: 10.3389/ijph.2026.1608765

3. Zhao Y, Yue R. White adipose tissue in type 2 diabetes and the effect of antidiabetic drugs. *Diabetol Metab Syndr* (2025) 17(1):116. doi: 10.1186/s13098-025-01678-9

4. Cifarelli V, Beeman SC, Smith GI, Yoshino J, Morozov D, Beals JW, et al. Decreased adipose tissue oxygenation associates with insulin resistance in individuals with obesity. *J Clin Invest* (2020) 130(12):6688–99. doi: 10.1172/JCI141828

5. Statello L, Guo CJ, Chen LL, Huarte M. Gene regulation by long non-coding RNAs and their biological functions. *Nat Rev Mol Cell Biol* (2021) 22(2):96–118. doi: 10.1038/s41580-020-00315-9

6. Ayub ALP, Tonin BCB, Azevedo H, Jordão PHF, Saxena T, Sejour L, et al. LncRNA Dlx4os drives malignant transformation and phenotype switching in melanoma. *Epigenetics* (2026) 21(1):2641924. doi: 10.1080/15592294.2026.2641924

7. Mattick JS, Amaral PP, Carninci P, Carpenter S, Chang HY, Chen LL, et al. Long non-coding RNAs: definitions, functions, challenges and recommendations. *Nat Rev Mol Cell Biol* (2023) 24(6):430–47. doi: 10.1038/s41580-022-00566-8

8. Gao H, Kerr A, Jiao H, Hon CC, Rydén M, Dahlman I, et al. Long non-coding RNAs associated with metabolic traits in human white adipose tissue. *EBioMedicine* (2018) 30:248–60. doi: 10.1016/j.ebiom.2018.03.010

9. Lluch A, Latorre J, Oliveras-Cañellas N, Fernández-Sánchez A, Moreno-Navarrete JM, Castells-Nobau A, et al. A novel long non-coding RNA connects obesity to impaired adipocyte function. *Mol Metab* (2024) 90:102040. doi: 10.1016/j.molmet.2024.102040

10. O'Reilly ME, Ho S, Coronel J, Zhu L, Liu W, Xue C, et al. linc-ADAIN, a human adipose lincRNA, regulates adipogenesis by modulating KLF5 and IL-8 mRNA stability. *Cell Rep* (2024) 43(5):114240. doi: 10.1016/j.celrep.2024.114240

11. Hong P, Wang D, Wu Y, Zhang Q, Liu P, Pan J, et al. A novel long noncoding RNA AK029592 contributes to thermogenic adipocyte differentiation. *Stem Cells Transl Med* (2024) 13(10):985–1000. doi: 10.1093/stcltm/szae056

12. Piórkowska K, Zygmunt K, Hunter W, Wróblewska K. MALAT1: a long non-coding RNA with multiple functions and its role in processes associated with fat deposition. *Genes* (2024) 15(4):479. doi: 10.3390/genes15040479

13. Dey BK, Banerjee S, Adhikary P, Chowdhury S, Roy S, Roy SB, et al. Expression of long non-coding RNAs MALAT1, MEG3, and XIST in gestational diabetes mellitus: a cross-sectional study. *Acta Diabetol* (2025) 63(1):105–14. doi: 10.1007/s00592-025-02581-5

14. Desiderio A, Pastorino M, Campitelli M, Prevenzano I, De Palma FDE, Spinelli R, et al. Hypomethylation at PANDAR promoter progressively induces senescence in adipocyte precursor cells in subjects with obesity and type 2 diabetes. *FASEB J Off Publ Fed Am Soc Exp Biol* (2024) 38(19):e70093. doi: 10.1096/fj.202401470R

15. Bäckdahl J, Franzén L, Massier L, Li Q, Jalkanen J, Gao H, et al. Spatial mapping reveals human adipocyte subpopulations with distinct sensitivities to insulin. *Cell Metab* (2021) 33(9):1869–82.e6. doi: 10.1016/j.cmet.2021.07.018

16. Fryk E, Olausson J, Mossberg K, Strindberg L, Schmelz M, Brogren H, et al. Hyperinsulinemia and insulin resistance in the obese may develop as part of a

homeostatic response to elevated free fatty acids: a mechanistic case-control and a population-based cohort study. *EBioMedicine* (2021) 65:103264. doi: 10.1016/j.ebiom.2021.103264

17. Wrench E, Subar DA, Bampouras TM, Lauder RM, Gaffney CJ. Myths and methodologies: assessing glycaemic control and associated regulatory mechanisms in human physiology research. *Exp Physiol* (2024) 109(9):1461–77. doi: 10.1113/EP091433

18. Bolger AM, Lohse M, Usadel B. Trimmomatic: a flexible trimmer for illumina sequence data. *Bioinformatics* (2014) 30(15):2114–20. doi: 10.1093/bioinformatics/btu170

19. Dobin A, Davis CA, Schlesinger F, Drenkow J, Zaleski C, Jha S, et al. STAR: ultrafast universal RNA-seq aligner. *Bioinformatics* (2013) 29(1):15–21. doi: 10.1093/bioinformatics/bts635

20. Mudge JM, Carbonell-Sala S, Diekhans M, Martinez JG, Hunt T, Jungreis I, et al. GENCODE 2025: reference gene annotation for human and mouse. *Nucleic Acids Res* (2025) 53(D1):D966–75. doi: 10.1093/nar/gkae1078

21. Liao Y, Smyth GK, Shi W. featureCounts: an efficient general-purpose program for assigning sequence reads to genomic features. *Bioinformatics* (2014) 30(7):923–30. doi: 10.1093/bioinformatics/btt656

22. Love MI, Huber W, Anders S. Moderated estimation of fold change and dispersion for RNA-seq data with DESeq2. *Genome Biol* (2014) 15(12):550. doi: 10.1186/s13059-014-0550-8

23. Anderson MJ. A new method for non-parametric multivariate analysis of variance. *Austral Ecol* (2001) 26(1):32–46. doi: 10.1111/j.1442-9993.2001.01070.pp.x

24. Errafii K, Boujraf S, Chikri M. Transcriptomic analysis from normal glucose tolerance to T2D of Obese individuals using bioinformatic tools. *Int J Mol Sci* (2023) 24(7):6337. doi: 10.3390/ijms24076337

25. Errafii K, Khalifa O, Al-Akl NS, Arredouani A. Comparative transcriptome analysis reveals that Exendin-4 improves steatosis in HepG2 cells by modulating signaling pathways related to lipid metabolism. *Biomedicines* (2022) 10(5):1020. doi: 10.3390/biomedicines10051020

26. Banaszak M, Górna I, Drzymała-Czyż S. Fatty acid profile and desaturase activity in obesity: roles, mechanisms, and clinical relevance. *Metabolites* (2025) 15(9):595. doi: 10.3390/metabo15090595

27. Orešanská K, Chomová M, Kubincová J, Turecký L, Ďurfinová M. Tissue-Specific differences in fatty acid content and desaturase activity between the liver and spinal cord of diabetic ZDF rats. *Biology* (2025) 14(9):1205. doi: 10.3390/biology14091205

28. Lee J, Saha PK, Yang QH, Lee S, Park JY, Suh Y, et al. Targeted inactivation of MLL3 histone H3–Lys-4 methyltransferase activity in the mouse reveals vital roles for MLL3 in adipogenesis. *Proc Natl Acad Sci* (2008) 105(49):19229–34. doi: 10.1073/pnas.0810100105

29. Escoté X, Aranda GB, Mora M, Casals G, Enseñat J, Vidal O, et al. Zinc alpha-2 glycoprotein is overproduced in Cushing's syndrome. *Endocrinol Diabetes Nutr* (2017) 64(1):26–33. doi: 10.1016/j.endinu.2016.10.002

30. Cilenti L, Di Gregorio J, Mahar R, Liu F, Ambivero CT, Periasamy M, et al. Inactivation of mitochondrial MUL1 E3 ubiquitin ligase deregulates mitophagy and prevents diet-induced obesity in mice. *Front Mol Biosci* (2024) 11:1397565. doi: 10.3389/fmolb.2024.1397565

31. Engin A. Adipose tissue hypoxia in obesity: clinical reappraisal of hypoxia hypothesis. *Adv Exp Med Biol* (2024) 1460:329–56. doi: 10.1007/978-3-031-63657-8_11

32. Li R, Zhu R, Yang X, Feng Y, He Q, Wang H, et al. The role of lncFABP4 in modulating adipogenic differentiation in buffalo intramuscular preadipocytes. *Anim Sci J Nihon Chikusan Gakkaiho* (2024) 95(1):e13951. doi: 10.1111/asj.13951

33. Wang Y, Tai YL, Way G, Zeng J, Zhao D, Su L, et al. RNA binding protein HuR protects against NAFLD by suppressing long noncoding RNA H19 expression. *Cell Biosci* (2022) 12(1):172. doi: 10.1186/s13578-022-00910-7

34. Zhang LH, Wang J, Tan BH, Yin YB, Kang YM. The association of lncRNA and mRNA changes in adipose tissue with improved insulin resistance in type 2 Obese diabetes mellitus rats after Roux-en-Y gastric bypass. *Dis Markers* (2022) 2022:8902916. doi: 10.1155/2022/8902916

35. Chen Y, Chen H, Wang Y, Liu F, Fan X, Shi C, et al. LncRNA LINK-A remodels tissue inflammatory microenvironments to promote obesity. *Adv Sci* (2024) 11(10):e2303341. doi: 10.1002/advs.202303341

36. Zhang Z, Cui Y, Su V, Wang D, Tol MJ, Cheng L, et al. A PPARγ/long noncoding RNA axis regulates adipose thermoneutral remodeling in mice. *J Clin Invest* (2023) 133(21):e170072. doi: 10.1172/JCI170072

37. Kerr AG, Wang Z, Wang N, Kwok KHM, Jalkanen J, Ludzki A, et al. The long noncoding RNA ADIPINT regulates human adipocyte metabolism *via* pyruvate carboxylase. *Nat Commun* (2022) 13(1):2958. doi: 10.1038/s41467-022-30620-0

38. García-Serrano S, Moreno-Santos I, Garrido-Sánchez L, Gutierrez-Repiso C, García-Almeida JM, García-Arnés J, et al. Stearoyl-CoA Desaturase-1 is associated with insulin resistance in morbidly Obese subjects. *Mol Med* (2011) 17(3–4):273–80. doi: 10.2119/molmed.2010.00078